Journal of Nonlinear Modeling and Analysis
Volume 8, Number 2, April 2026, 608–640
https://global-sci.com/jnma
DOI:10.12150/jnma.2026.608

Steady State Solution and Its Stability Analysis of a Reaction-Diffusion Mathematical Model for LDL, Lipoprotein(a), and CRP in Atherosclerosis

Aytekin Enver[1,†] and Fatma Ayaz[2]

Received 9 July 2025; Accepted 1 September 2025

Abstract This study presents a reaction-diffusion mathematical model to investigate the spatiotemporal dynamics of low-density lipoprotein (LDL), lipoprotein(a), and C-reactive protein (CRP) within the arterial wall, key mediators in the pathogenesis of atherosclerosis and related cardiovascular diseases. The model employs a system of partial differential equations to capture both the diffusion of these biomolecules and their biochemical interactions, including LDL oxidation, CRP-mediated inflammatory responses, and plaque initiation. Numerical simulations, implemented using the finite difference method, demonstrate that CRP substantially accelerates LDL oxidation and promotes plaque deposition, particularly in regions of locally elevated lipoprotein concentrations. Furthermore, the results indicate that elevated CRP levels synergistically enhance the pro-atherogenic effects of LDL and lipoprotein(a), highlighting the critical role of inflammation in plaque progression. These findings underscore the potential of anti-inflammatory therapeutic strategies, alongside lipid-lowering interventions, in mitigating atherosclerotic risk. The proposed model provides a robust computational framework for elucidating the interactive effects of lipid metabolism and vascular inflammation in the progression of cardiovascular disease.

Keywords Finite difference, reaction-diffusion, LDL, C-reactive protein (CRP), lipoprotein(a)

MSC(2010) 65M06, 35K57, 93A30, 92B10.

1. Introduction

Atherosclerosis is a significant cardiovascular disease responsible for high mortality worldwide [1–4]. As illustrated in Figure 1, the process begins when low-density lipoprotein (LDL) penetrates the intimal layer of the arterial wall, initiating an inflammatory response that eventually leads to the formation of fibrous plaques. Fat buildup is a more complicated process described as an inflammatory response type 1, creating oxidative stress in the artery wall, which lays down plaques that obstruct blood flow. Low-density lipoprotein (LDL), lipoprotein(a), and C-reactive protein (CRP) drive lipid peroxidation, inflammation and spurring the development

[†]The corresponding author.
Email address: aytekinanwer@gmail.com (Aytekin Enver), fayaz@gazi.edu.tr (Fatma Ayaz)
[1]Graduate School of Natural and Applied Sciences, Department of Mathematics, Gazi University, Besevler, 06550, Türkiye
[2]Department of Mathematics, Gazi University, Besevler, 06550, Türkiye

leading accelerators of the atherosclerotic process. We will explore and discuss these mechanisms as well as disease progression, and potential therapeutic interventions according to mathematical model frameworks. An important trend for the simulation of atherosclerosis is the use of reaction–diffusion models that consider both molecular and biochemical levels [5–7].

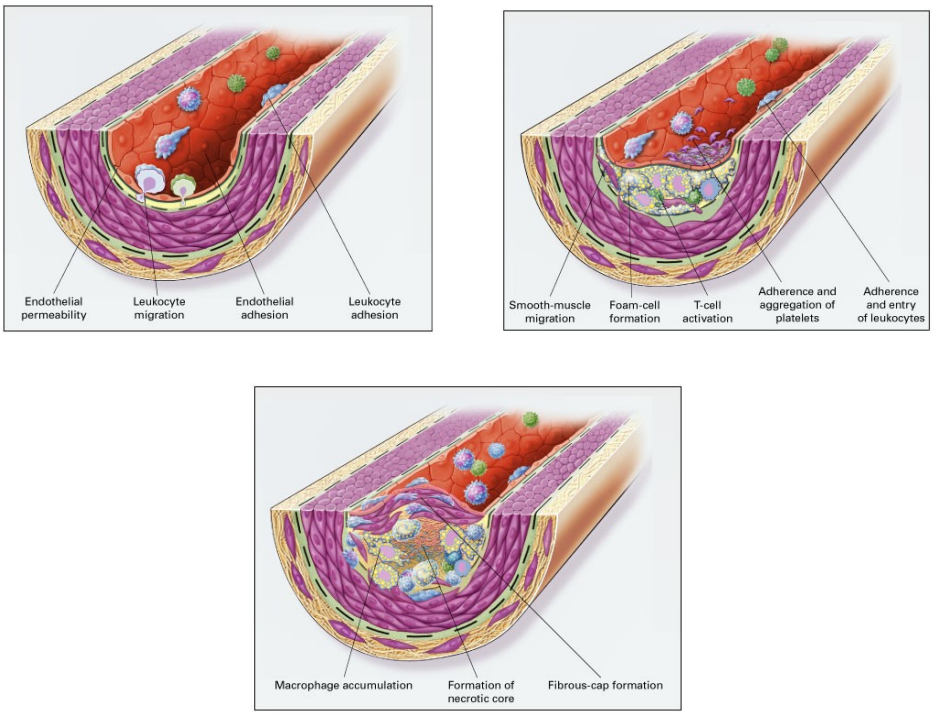

Figure 1. Early events of atherosclerosis. LDL penetrates in the intima, thus triggering an inflammatory process. The atheromatous plaque is eventually covered by a fibrous cap made of smooth muscle cells [8].

The atherosclerosis inflammatory processes have been modeled mathematically [9, 10]. The governing equations used in low-density lipoprotein (LDL) oxidation were either ordinary differential equation (ODE) [11,12] or partial differential equation (PDE) [13–17].

Research revealed the importance of high-density lipoprotein and C-reactive protein in forming atherosclerotic plaques. Low-density lipoprotein, often referred to as "bad cholesterol" is a lipoprotein that transports cholesterol to peripheral tissues where it can accumulate in the arteries and oxidize.

Oxidized low-density lipoprotein (Ox-LDL) is especially bad because it leads to the development of atherosclerotic plaques: Ox-LDL triggers an inflammatory response, recruiting immune cells like macrophages to take up the LDL and morph into foam cells (iconic in their plaque-harboring stature). C-reactive protein, an acute phase reactant that is released in circulation during infection and inflammation and which promotes low density lipoprotein oxidation, as above, also plays a key role in platelet activation (via transcription-induced arachidonic acid release), and the immune response to damaged endothelial tissue: C-reactive lipoprotein released by macrophages enhances monocyte chemotactic sites in plaque-mediated

recruitment of peripheral antibody-producing cells.

Moreover, this situation can be complicated by lipoprotein (a), the genetic variant of low-density lipoprotein, which has one more atherogenic potential to produce low density lipoprotein (an integer that is multiplied if C-reactive protein is high) [18–21].

To explore these intricate pathways, mathematical models that include diffusion and reaction mechanisms are ideal. Interaction & diffusion examples describe how molecules like LDL, CRP, and lipoprotein(a) diffuse through arterial walls (diffusion) and how they interact. These parameters (such as the diffusion coefficient, which diffuses into the medium) affect the control of this diffusion process. The word reaction refers to the biochemical process that occurs between molecules, such as the oxidation of LDL by CRP or the formation of foam cells from macrophages. Using this system of partial differential equations to solve the system describes locally and temporally how atherosclerosis emerges, develops, and progresses, providing invaluable insight into the evolution of such a disease [22, 23].

One of the principal numerical methods used to solve partial differential equations is the finite difference method [24, 25]. Converting continuous functions to discrete values means calculating changes over time and space little by little. The model could be used to track the diffusion of LDL, CRP and lipoprotein(a) across arterial walls in atherosclerosis, and their interactions.

But it is reactive with other cells, such as macrophages and foam cells. By incorporating clinical data with this model, it becomes possible to simulate an atherosclerosis progression that is grounded, generating a comprehensive perspective of the lifecycle of plaque initiation and growth integrated throughout time.

To address all these studies, we aimed to obtain a complete and accurate picture, and therefore the purpose of this study is to create a reaction-diffusion model which can also include LDL, CRP and lipoprotein(a). This is a model written with finite difference method which simulates the diffusion and interaction of biomolecules into arterial walls and studies carefully the roles they play in plaque formation and growth. In addition, the model will leverage clinical phenotyping of patients with diabetes to dissect how hyperglycemia and insulin resistance act as drivers of atherosclerosis progression, and underscore why lipid lowering or anti-inflammatory drugs should be tailored according to their ability to target alterations in lipid metabolism and inflammation that are specific to individual diabetic individuals [26, 27].

Recent contributions in the literature, including the work of Xuming Xie, present a study that aims to further the reaction-diffusion approach, testing a model with an extended variable spectrum and taking into account some essential factors in this context (lipoprotein(a) and C-reactive protein) that are pivotal for the understanding of the inflammatory and oxidative mechanisms underlying atherosclerosis in diabetic patients. Through integration of mathematical models and clinical concepts, the study aims a basic understanding of atherosclerotic molecular mechanisms, which might help develop innovative therapeutic strategies. [28–30].

In recent years, mathematical modeling of complex biomedical processes has increasingly employed reaction-diffusion and fractional diffusion frameworks to capture spatio-temporal disease dynamics with high fidelity. For example, *in silico* simulations of amyloid-beta aggregation and senile plaque formation in Alzheimer's disease have revealed the critical role of neuroinflammation and oxidative stress in plaque progression, providing insights for therapeutic interventions. Similarly, frac-

tional Proliferation-Invasion models have been effectively used to predict glioblastoma multiforme (GBM) growth based on early-stage MRI data, enabling patient-specific predictions and facilitating the optimization of treatment strategies. Fractional diffusion equations have also been successfully applied to model viral propagation, such as SARS-CoV-2 transport in tissue and groundwater, demonstrating the importance of nonlocal and memory-dependent effects in biological transport phenomena. Inspired by these approaches, our study extends the reaction-diffusion paradigm to the context of atherosclerosis, modeling the coupled diffusion and biochemical interactions of LDL, lipoprotein(a), and CRP to provide mechanistic insights into plaque initiation, inflammatory amplification, and the potential impact of targeted therapeutic interventions [31–35].

2. Mathematical model

2.1. Problem definition and mathematical preliminaries

In this section, we provide a comprehensive mathematical description of our model and present the necessary preliminaries for the subsequent analysis in detail. Our goal is to explicitly state all the components of our reaction-diffusion system and their interactions, thereby establishing a solid foundation for the analysis steps that follow.

Reaction-diffusion equations are widely used for modeling chemical reactions, biological systems, population dynamics, and nuclear reactor physics. They are of the form:

$$\frac{\partial u}{\partial t} = D\Delta u + f(u, \lambda), \tag{2.1}$$

where $u = (u_1, \ldots, u_k)$ represents various substances in a chemical reaction or species of a biological system; $\lambda \in \mathbb{R}^p$ is a vector of control parameters; Δ is the Laplace operator in the spatial variables; and $D \in \mathbb{R}^{k\times k}$ is a symmetric and semi-positive definite matrix. They describe diffusion of different substances. The matrix D is often diagonal and corresponds to the diffusion rates of the substances. The function $f : \mathbb{R}^k \times \mathbb{R}^p \longrightarrow \mathbb{R}^k$ is a vector of smooth functions and represents the reaction among the substances.

The proposed model represents how three fundamental biochemical components distribute and interact in space and time through a reaction-diffusion system. These components are:

- Low-Density Lipoprotein (LDL) concentration, denoted by $L(x, t)$;
- Lipoprotein(a) concentration, denoted by $P(x, t)$;
- C-Reactive Protein (CRP) concentration, denoted by $C(x, t)$.

The system models the diffusion and reactions of these components within biological tissue using the following partial differential equations:

2.2. Governing equations

For LDL equation:
The reaction-diffusion equation for LDL is:

$$\frac{\partial L}{\partial t} = D_L\Delta L - k_1 LC - k_2 LP + r_1, \quad x \in \Omega,\ t > 0. \tag{2.2}$$

Here, $(D_L \Delta L)$ represents the diffusion of LDL in the arterial wall. $(-k_1 LC)$ represents the reaction where CRP accelerates the oxidation of LDL. $(-k_2 LP)$ represents the interaction between lipoprotein(a) and LDL, where this interaction accelerates LDL oxidation. (r_1) represents the continuous production of LDL in the body.

For lipoprotein(a) equation:

$$\frac{\partial P}{\partial t} = D_P \Delta P - k_3 PC + r_2, \quad x \in \Omega,\ t > 0. \tag{2.3}$$

Here, $(D_P \Delta P)$ represents the diffusion of lipoprotein(a) in the arterial wall. $(-k_3 PC)$ represents the reaction where CRP interacts with lipoprotein(a), making it more atherogenic. (r_2) represents the continuous production of lipoprotein(a).

For CRP equation:

$$\frac{\partial C}{\partial t} = D_C \Delta C + f(C) - k_4 CL + r_3, \quad x \in \Omega,\ t > 0.$$

Here, $(D_C \Delta C)$ represents the diffusion of CRP in the arterial wall. $f(C)$ represents CRP's pro-inflammatory effect and a positive feedback mechanism (e.g., CRP promoting its own production). We will take it as aC^2. $(-k_4 CL)$ represents the interaction between LDL and CRP, which increases oxidative stress. (r_3) represents the production of CRP during inflammation. Thus, the equation becomes:

$$\frac{\partial C}{\partial t} = D_C \Delta C + aC^2 - k_4 CL + r_3, \quad x \in \Omega,\ t > 0. \tag{2.4}$$

2.3. Initial and boundary conditions

Initial conditions:
The initial spatial distribution of each component is given by:

$$L(x,0) = L_0(x), \quad P(x,0) = P_0(x), \quad C(x,0) = C_0(x), \quad x \in \Omega,$$

where $L_0(x),\ P_0(x),\ C_0(x)$ are positive functions defined in the $H^1(\Omega)$ space.

Boundary conditions:
We apply homogeneous Neumann boundary conditions at the domain boundary:

$$\frac{\partial L}{\partial n} = 0, \quad \frac{\partial P}{\partial n} = 0, \quad \frac{\partial C}{\partial n} = 0, \quad \partial(x) \in \Omega,\ t > 0.$$

These conditions indicate that there is no flux of components across the boundary of the domain.

Domain definition:
The domain is defined as $\Omega \subset \mathbb{R}^n$, which is a bounded, connected domain with a smooth (Lipschitz continuous) boundary. The spatial dimension is $n = 1, 2, 3$; in biological applications, three dimensions are often considered.

3. Uniqueness and existence

The inclusion of Sections 3–5, which focus on the existence and uniqueness of solutions, stability analysis, and semi-analytical validation, is essential to ensure that the observed spatio-temporal behaviors are not only numerical artifacts but also mathematically rigorous and biologically interpretable. This theoretical foundation guarantees that the exponential decay and growth patterns shown in the results reflect the intrinsic properties of the proposed reaction-diffusion system.

We will prove the existence of a weak solution using the Galerkin method, energy estimates, and compactness arguments.

3.1. Galerkin approach

Let $\{\phi_i\}_{i=1}^{\infty}$ be an orthonormal basis of $H^1(\Omega)$ with respect to the $L^2(\Omega)$ inner product [22]. For each $N \in \mathbb{N}$, define the finite-dimensional subspace:

$$V_N = \text{span}\{\phi_1, \phi_2, \ldots, \phi_N\}.$$

We seek approximate solutions $L^N, P^N, C^N \in V_N$:

$$L^N(x,t) = \sum_{i=1}^{N} l_i(t)\phi_i(x), \tag{3.1}$$

$$P^N(x,t) = \sum_{i=1}^{N} p_i(t)\phi_i(x), \tag{3.2}$$

$$C^N(x,t) = \sum_{i=1}^{N} c_i(t)\phi_i(x), \tag{3.3}$$

where $l_i(t),\ p_i(t),\ c_i(t)$ are unknown coefficient functions.

3.2. Derivation of the Galerkin system

We multiply each equation by $\phi_j(x)$ and integrate over Ω:

$$\left(\frac{\partial L^N}{\partial t}, \phi_j(x)\right) = -D_L(\nabla L^N, \nabla\phi_j) - k_1(L^N C^N, \phi_j) - k_2(L^N P^N, \phi_j) + (r_1, \phi_j), \tag{3.4}$$

$$\left(\frac{\partial P^N}{\partial t}, \phi_j(x)\right) = -D_P(\nabla P^N, \nabla\phi_j) - k_3(P^N C^N, \phi_j) + (r_2, \phi_j), \tag{3.5}$$

$$\left(\frac{\partial C^N}{\partial t}, \phi_j(x)\right) = -D_C(\nabla C^N, \nabla\phi_j) + a((C^N)^2, \nabla\phi_j) - k_4(C^N L^N, \phi_j) + (r_3, \phi_j), \tag{3.6}$$

for $j = 1, 2, \ldots, N$, where $(\cdot,\cdot)$ denotes the $L^2(\Omega)$ inner product.

The direct solution of partial differential equations (PDEs), such as reaction-diffusion systems, is generally difficult because these equations are defined in infinite-dimensional function spaces. Therefore, to demonstrate the existence and uniqueness of solutions for such equations, the problem needs to be reduced to a more manageable form [36–38].

3.3. Local existence

Since the functions F^N are continuous and locally Lipschitz in u^N, the Picard-Lindelöf theorem ensures local existence and uniqueness of solutions to the ODE system [23].

Initial conditions:

$$L^N(x,0) = L_0^N(x), \quad P^N(x,0) = P_0^N(x), \quad C^N(x,0) = C_0^N(x),$$

where L_0^N, P_0^N, C_0^N are the orthogonal projections of L_0, P_0, C_0 onto V_N.

A priori estimates:
We define the energy functional as

$$E^N(t) = \frac{1}{2}\int_\Omega \left((L^N)^2 + (P^N)^2 + (C^N)^2\right) dx. \tag{3.7}$$

Now, we compute the time derivative:

$$\frac{dE^N}{dt} = \int_\Omega \left(L^N \frac{\partial L^N}{\partial t} + P^N \frac{\partial P^N}{\partial t} + C^N \frac{\partial C^N}{\partial t}\right) dx. \tag{3.8}$$

Substituting the expressions from the Galerkin equations [36], we obtain

$$\begin{aligned}\frac{dE^N}{dt} =& - D_L \int_\Omega |\nabla L^N|^2 dx - D_P \int_\Omega |\nabla P^N|^2 dx - D_C \int_\Omega |\nabla C^N|^2 dx \\ & - k_1 \int_\Omega (L^N)^2 C^N dx - k_2 \int_\Omega (L^N)^2 P^N dx - k_3 \int_\Omega (P^N)^2 C^N dx \\ & + a \int_\Omega (C^N)^3 dx - k_4 \int_\Omega (L^N)^2 dx + \int_\Omega \left(r_1 L^N + r_2 P^N + r_3 C^N\right) dx. \end{aligned} \tag{3.9}$$

Estimation of nonlinear terms:
We use Hölder's and Sobolev inequalities [39,40]. Applying Hölder's inequality, we obtain

$$\int_\Omega |L^N|^2 C^N dx \le \|L^N\|^2_{L^4(\Omega)} \, \|C^N\|_{L^2(\Omega)}. \tag{3.10}$$

From the Sobolev embedding $H^1(\Omega) \hookrightarrow L^4(\Omega)$:

$$\|L^N\|_{L^4(\Omega)} \le C \|L^N\|_{H^1(\Omega)}.$$

Now apply Young's inequality for any $\varepsilon > 0$:

$$\|L^N\|^2_{L^4(\Omega)} \le \varepsilon \|\nabla L^N\|^2_{L^2(\Omega)} + C_\varepsilon \|L^N\|^2_{L^2(\Omega)}. \tag{3.11}$$

Similar estimates can be derived for other nonlinear terms involving P^N and C^N.

Estimation of $-k_2 \int_\Omega (L^N)^2 P^N \, dx$:
We need to estimate the term:

$$\int_\Omega |L^N|^2 |P^N| \, dx.$$

Applying Hölder's Inequality:

$$\int_\Omega |L^N|^2 |P^N|\, dx \leq \|L^N\|^2_{L^4(\Omega)} \, \|P^N\|_{L^2(\Omega)}. \tag{3.12}$$

By Sobolev Embedding: since $H^1(\Omega) \hookrightarrow L^4(\Omega)$ for $n \leq 3$,

$$\|L^N\|_{L^4(\Omega)} \leq C \|L^N\|_{H^1(\Omega)}.$$

Applying Young's Inequality, for any $\varepsilon > 0$,

$$\|L^N\|^2_{L^4(\Omega)} \leq \varepsilon \|\nabla L^N\|^2_{L^2(\Omega)} + C_\varepsilon \|L^N\|^2_{L^2(\Omega)}. \tag{3.13}$$

Combining the estimates we substitute back into the original term:

$$\int_\Omega |L^N|^2 |P^N|\, dx \leq \varepsilon \|\nabla L^N\|^2_{L^2(\Omega)} + C_\varepsilon \|L^N\|^2_{L^2(\Omega)} \, \|P^N\|_{L^2(\Omega)}. \tag{3.14}$$

This term can now be controlled in the energy inequality by absorbing $\|\nabla L^N\|^2_{L^2(\Omega)}$ into the left-hand side and bounding the remaining terms with the energy functional $E^N(t)$.

Estimation of $-k_3 \int_\Omega (P^N)^2 C^N \, dx$:
We need to estimate:

$$\int_\Omega |P^N|^2 |C^N|\, dx.$$

Applying Hölder's Inequality:

$$\int_\Omega |P^N|^2 |C^N|\, dx \leq \|P^N\|^2_{L^4(\Omega)} \, \|C^N\|_{L^2(\Omega)}. \tag{3.15}$$

By Sobolev Embedding: since $H^1(\Omega) \hookrightarrow L^4(\Omega)$,

$$\|P^N\|_{L^4(\Omega)} \leq C \|P^N\|_{H^1(\Omega)}.$$

Applying Young's Inequality, for any $\varepsilon > 0$,

$$\|P^N\|^2_{L^4(\Omega)} \leq \varepsilon \|\nabla P^N\|^2_{L^2(\Omega)} + C_\varepsilon \|P^N\|^2_{L^2(\Omega)}. \tag{3.16}$$

Combining the estimates, we obtain

$$\int_\Omega |P^N|^2 |C^N|\, dx \leq \varepsilon \|\nabla P^N\|^2_{L^2(\Omega)} + C_\varepsilon \|P^N\|^2_{L^2(\Omega)} \, \|C^N\|_{L^2(\Omega)}. \tag{3.17}$$

This term can be controlled similarly within the energy inequality.

3.4. Further estimation of nonlinear terms

Estimation of $a \int_\Omega (C^N)^3 \, dx$:
We need to estimate:

$$\int_\Omega (C^N)^3 dx.$$

Applying Hölder's Inequality:

$$\int_\Omega (C^N)^3 dx \leq \|C^N\|^3_{L^3(\Omega)}.$$

By Sobolev Embedding, since $H^1(\Omega) \hookrightarrow L^4(\Omega)$ for $n \leq 3$,

$$\|C^N\|_{L^3(\Omega)} \leq \|C^N\|_{L^6(\Omega)} \leq C\|C^N\|_{H^1(\Omega)}.$$

Combining the estimates, we obtain

$$\int_\Omega (C^N)^3 dx \leq C\|C^N\|^3_{H^1(\Omega)}. \tag{3.18}$$

Applying Young's Inequality, for any $\varepsilon > 0$,

$$C\|C^N\|^3_{H^1(\Omega)} \leq \varepsilon\|\nabla C^N\|^2_{L^2(\Omega)} + C_\varepsilon\|C^N\|^6_{L^2(\Omega)}. \tag{3.19}$$

This term can be controlled in energy inequality.

Estimation of $-k_4 \int_\Omega (C^N)^2 L^N \, dx$:
We need to estimate:

$$\int_\Omega |C^N|^2 |L^N| dx.$$

Applying Hölder's Inequality:

$$\int_\Omega |C^N|^2 |L^N| dx \leq \|C^N\|^2_{L^4(\Omega)} \|L^N\|_{L^2(\Omega)}. \tag{3.20}$$

Using Sobolev Embedding:

$$\|C^N\|_{L^4(\Omega)} \leq C\|C^N\|_{H^1(\Omega)}.$$

Applying Young's Inequality:

$$\|C^N\|^2_{L^4(\Omega)} \leq \varepsilon\|\nabla C^N\|^2_{L^2(\Omega)} + C_\varepsilon\|C^N\|^2_{L^2(\Omega)}.$$

Combining the estimates:

$$\int_\Omega |C^N|^2 |L^N| dx \leq \varepsilon\|\nabla C^N\|^2_{L^2(\Omega)} + C_\varepsilon\|C^N\|^2_{L^2(\Omega)} \|L^N\|_{L^2(\Omega)}. \tag{3.21}$$

This term can be controlled in energy inequality.

By estimating all the nonlinear terms involving L^N, P^N, C^N using Hölder's inequality, Sobolev embeddings, and Young's inequality, we ensure that:

- the terms involving $\|\nabla L^N\|^2_{L^2(\Omega)}$, $\|\nabla P^N\|^2_{L^2(\Omega)}$ and $\|\nabla C^N\|^2_{L^2(\Omega)}$ can be absorbed into the left-hand side of the energy inequality by choosing $\varepsilon > 0$;
- the remaining terms are bounded by $E^N(t)$ and its higher powers.

Thus, the energy inequality takes the form:

$$\frac{dE^N}{dt} + \alpha \left(\|\nabla L^N\|^2_{L^2(\Omega)} + \|\nabla P^N\|^2_{L^2(\Omega)} + \|\nabla C^N\|^2_{L^2(\Omega)} \right) \leq C_1 E^N(t) + C_2 (E^N(t))^\gamma, \tag{3.22}$$

where $\alpha > 0$, $C_1, C_2 > 0$, and $\gamma > 0$.

Applying the nonlinear Gronwall inequality:
With the energy inequality established, we can show that $E^N(t)$ is bounded for all $t \geq 0$ and conclude the global existence of the approximate solutions. We will provide a detailed, step-by-step application of the nonlinear Gronwall inequality [25] to bound the energy functional $E^N(t)$ and demonstrate the global existence of the approximate solutions

$$u^N(t) = (L^N, P^N, C^N).$$

From the energy estimates, we have obtained the following differential inequality for the energy functional $E^N(t)$:

$$\frac{dE^N}{dt} \leq C_1 E^N(t) + C_2 (E^N(t))^\gamma, \tag{3.23}$$

where:

- $C_1, C_2 > 0$ are constants,
- $\gamma > 1$ arises from the nonlinear terms.

Now, we are setting up the differential inequality. Let

$$y(t) = E^N(t).$$

The inequality becomes:

$$\frac{dy}{dt} \leq C_1 y(t) + C_2 (y(t))^\gamma. \tag{3.24}$$

Recognize the type of inequality:
This is a first-order ordinary differential inequality of the form:

$$\frac{dy}{dt} \leq a y(t) + b (y(t))^\gamma, \tag{3.25}$$

with $a = C_1$ and $b = C_2$.

Applying the nonlinear Gronwall inequality:
The nonlinear Gronwall inequality [41] states that if $y(t)$ satisfies

$$\frac{dy}{dt} \leq f(y(t)),$$

where f is a continuous function, then under certain conditions on f we can bound $y(t)$.

In our case,

$$f(y) = C_1 y + C_2 y^\gamma.$$

To integrate, we consider the reciprocal of $f(y)$:

$$\frac{1}{f(y)} = \frac{1}{C_1 y + C_2 y^\gamma} = \frac{1}{y\big(C_1 + C_2 y^{\gamma-1}\big)}.$$

However, directly integrating this expression can be challenging due to the nonlinear term.

Comparison function:
Alternatively, consider a comparison function $z(t)$ satisfying

$$\frac{dz}{dt} = C_1 z(t) + C_2 (z(t))^\gamma,$$

with initial condition $z(0) = y(0)$. Since

$$\frac{dy}{dt} \leq \frac{dz}{dt}, \quad y(0) = z(0),$$

by the comparison theorem for ODEs, we have

$$y(t) \leq z(t) \quad \text{for all } t \geq 0.$$

Now, we rewrite the equation as

$$dt = \frac{dz}{C_1 z(t) + C_2 (z(t))^\gamma}.$$

This integral may not have a closed-form solution, but we can analyze the behavior of $z(t)$:

- If $z(t)$ remains bounded, then $y(t) \leq z(t)$ remains bounded.
- If $z(t)$ blows up in finite time, we need to investigate whether $y(t)$ also blows up.

Worst-case scenario:
Now assume $z(t)$ blows up at some finite time $T_{\max}$. Consider the worst-case scenario by neglecting the linear term:

$$\frac{dz}{dt} \leq C_2 (z(t))^\gamma.$$

This simplifies the inequality to

$$z^{-\gamma} dz \leq C_2 \, dt.$$

Integrating both sides:

$$\int_{z(0)}^{z(t)} z^{-\gamma} \, dz \leq C_2 \int_0^t dt,$$

$$\frac{1}{1-\gamma} \left[z(t)^{1-\gamma} - z(0)^{1-\gamma} \right].$$

Solving for $z(t)$:

$$z(t)^{1-\gamma} \geq z(0)^{1-\gamma} + (1-\gamma) C_2 t.$$

Since $\gamma > 1$, we have $1 - \gamma < 0$, so the right-hand side decreases in t. There exists a finite blow-up time $T_{\text{blow-up}}$ such that the right-hand side reaches zero:

$$z(0)^{1-\gamma} + (1-\gamma) C_2 T_{\text{blow-up}} = 0,$$

$$T_{\text{blow-up}} = \frac{z(0)^{1-\gamma}}{(1-\gamma) C_2}.$$

This suggests that $z(t)$ could blow up in finite time. However, in our original inequality, we have an additional linear term $C_1 y(t)$ and damping terms from the diffusion (the gradient norms), which we have neglected in this simplified analysis.

Role of diffusion:
In the full energy inequality, the diffusion terms $\|\nabla L^N\|^2_{L^2(\Omega)}$, $\|\nabla P^N\|^2_{L^2(\Omega)}$, and $\|\nabla C^N\|^2_{L^2(\Omega)}$ provide a damping effect that counteracts the potential blow-up caused by the nonlinear reaction terms. These diffusion terms prevent the solution from becoming unbounded in finite time.

From the energy inequality:

$$\frac{dE^N}{dt} + \alpha D^N(t) \leq C_1 E^N(t) + C_2 (E^N(t))^\gamma,$$

where

$$D^N(t) = \|\nabla L^N\|^2_{L^2(\Omega)} + \|\nabla P^N\|^2_{L^2(\Omega)} + \|\nabla C^N\|^2_{L^2(\Omega)}.$$

The presence of $D^N(t)$ on the left-hand side helps control the growth of $E^N(t)$. Now, given that the initial energy $E^N(0)$ is finite, and given the damping effect from diffusion, we can conclude that $E^N(t)$ remains bounded for all $t \geq 0$.

Since $E^N(t)$ remains bounded, the coefficients $l_i(t), p_i(t), c_i(t)$ in the ODE system remain bounded, and there is no finite-time blow-up. Therefore, the approximate solutions $L^N(x,t), P^N(x,t), C^N(x,t)$ exist for all $t \geq 0$. By applying the nonlinear Gronwall inequality and considering the damping effect of the diffusion terms, we have shown that the energy functional $E^N(t)$ remains bounded for all time, ensuring the global existence of the approximate solutions.

3.5. uniqueness

Theorem 3.1. *(Uniqueness of solutions for reaction-diffusion systems).*
Consider a reaction-diffusion system in a bounded domain $\Omega \subset \mathbb{R}^n$ with smooth boundary, described by:

$$\frac{\partial u_i}{\partial t} = D_i \Delta u_i + f_i(u_1, u_2, \ldots, u_m), \quad \text{in } \Omega \times (0,T], \quad i = 1,2,3,\ldots,m$$

subject to initial conditions

$$u_i(x,0) = u_{i0}(x), \quad x \in \Omega,$$

and appropriate boundary conditions (e.g., homogeneous Neumann or Dirichlet).

Assumptions:

- Initial Data: $u_{i0} \in H^1(\Omega)$ are given functions.
- Diffusion Coefficients: $D_i > 0$ for each i.
- Reaction Terms: Functions f_i are locally Lipschitz continuous with respect to $(u_1, u_2, \ldots, u_m)$.

Under these conditions, the reaction-diffusion system admits a unique weak solution

$$\mathbf{u} = (u_1, u_2, \ldots, u_m)$$

in an appropriate function space.

Now we express the nonlinear terms:

$$L_1C_1 - L_2C_2 = L_1\delta C + \delta L C_2,$$

$$L_1P_1 - L_2P_2 = L_1\delta P + \delta L P_2,$$

$$P_1C_1 - P_2C_2 = P_1\delta C + \delta P C_2,$$

$$C_1^2 - C_2^2 = (C_1 + C_2)\delta C,$$

$$C_1L_1 - C_2L_2 = C_1\delta L + \delta C L_2.$$

After substituting and simplifying, we obtain:

$$\begin{aligned}\frac{dE}{dt} =& - D_L \int_\Omega |\nabla \delta L|^2 \, dx - D_P \int_\Omega |\nabla \delta P|^2 \, dx - D_C \int_\Omega |\nabla \delta C|^2 \, dx \\ & - k_1 \int_\Omega \delta L (L_1 \delta C + \delta L C_2) \, dx - k_2 \int_\Omega \delta L (L_1 \delta P + \delta L P_2) \, dx \\ & - k_3 \int_\Omega \delta P (P_1 \delta C + \delta P C_2) \, dx + a \int_\Omega \delta C (C_1 + C_2) \delta C \, dx \\ & - k_4 \int_\Omega \delta C (C_1 \delta L + \delta C L_2) \, dx.\end{aligned} \tag{3.26}$$

Since $L_1, P_1, C_1, L_2, P_2, C_2$ are bounded in $L^\infty(\Omega \times (0,T))$ due to the existence proof, we can denote:

$$M = \|L_i\|_{L^\infty}, \|P_i\|_{L^\infty}, \|C_i\|_{L^\infty}, \quad i = 1, 2.$$

We estimate the nonlinear terms using Cauchy-Schwarz and Young's inequalities. For the term involving k_1:

$$\begin{aligned}k_1 \int_\Omega \delta L \left(L_1 \delta C + \delta L C_2\right) dx =& - k_1 \int_\Omega \delta L L_1 \delta C \, dx - k_1 \int_\Omega (\delta L)^2 C_2 \, dx \\ \leq& k_1 M \|\delta L\|_{L^2} \|\delta C\|_{L^2} + \|\delta L\|_{L^2}^2.\end{aligned} \tag{3.27}$$

Similar estimates can be made for the other nonlinear terms. Now, gather all the terms to obtain:

$$\frac{dE}{dt} \leq -\alpha \left(\|\nabla \delta L\|_{L^2}^2 + \|\nabla \delta P\|_{L^2}^2 + \|\nabla \delta C\|_{L^2}^2 \right) + K E(t), \tag{3.28}$$

where $\alpha > 0$, $K > 0$ depend on M and the reaction coefficients.

Since the gradient terms are non-negative, we can drop them to obtain

$$\frac{dE}{dt} \leq K E(t).$$

Using Gronwall's inequality:

$$E(t) \leq E(0) e^{Kt}.$$

Since the solutions have the same initial data:

$$\delta L(x,0) = 0, \quad \delta P(x,0) = 0, \quad \delta C(x,0) = 0 \quad \Longrightarrow \quad E(0) = 0,$$

we obtain

$$E(t) \leq 0 \cdot e^{Kt} = 0$$

almost everywhere in $\Omega \times [0, T]$.

Thus,

$$(L_1, P_1, C_1) = (L_2, P_2, C_2).$$

Under the given assumptions, the weak solution L, P, C to the reaction-diffusion system is unique.

4. Stability for the reaction-diffusion equations

According to W. B. Fitzgibbon and his collaborators, stability analysis is closely associated with reaction-diffusion equations and the modeling of biological processes. Stability in reaction-diffusion systems is especially important for understanding dynamic equilibrium in biological systems. Such models are used to study how biochemical processes develop and the existence of stationary solutions. Stationary solutions of the system represent situations in which, under certain parameters, the model will remain constant without temporal variations.

Theorem 4.1. *The equilibrium point $x = 0$ of $\dot{x} = Ax$ is stable if and only if all eigenvalues of A satisfy $\Re(\lambda_i) \leq 0$ and for every eigenvalue with $\Re(\lambda_i) = 0$ and algebraic multiplicity $q_i \geq 2$,*

$$\operatorname{rank}(A - \lambda_i I) = n - q_i,$$

where n is the dimension of x. The equilibrium point $x = 0$ is (globally) asymptotically stable if and only if all eigenvalues of A satisfy $\Re(\lambda_i) < 0$ [10].

The reaction-diffusion equations in the mathematical modeling section are used to study the interactions of species and diffusion processes in biological systems. Stability analysis determines how the solutions of these equations behave time-dependently and whether they reach a stationary equilibrium within a given range of parameters. Ensuring stability plays a critical role in biological equilibrium and in understanding the long-term behavior of the system.

Stability analysis for reaction-diffusion systems is generally based on testing whether stationary solutions are stable to small perturbations. If slight changes allow the system to revert to its stationary solution, that solution is stable; however, if the system deviates from a different solution, this solution is unstable [9].

An appropriate Lyapunov function is selected for stability analysis. This function must be defined in such a way that all variables in the system are positive definite and minimal in the equilibrium state of the system.

The form of Lyapunov functions is usually as follows:

$$V(u) = \sum_{i=1}^{m} V_i(u_i). \tag{4.1}$$

Here V_i is a function that measures the distance of each component to the equilibrium state. The negative derivative of this function guarantees the stability of the system. The derivative of the system with respect to the Lyapunov function

is used to analyze the stability of the equilibrium state. If the derivative is negative, the system is stable:

$$\dot{V} = \sum_{i=1}^{m} \frac{\partial V}{\partial u_i} f_i(u) \leq 0. \tag{4.2}$$

Here, $f_i(u)$ is the function on the right-hand side of the reaction-diffusion equation for each component of the system.

The important thing here is that if the derivative of the Lyapunov function is negative, the system will be asymptotically stable. This means that the system will return to a state of equilibrium after a small perturbation. To ensure asymptotic stability, we also require:

$$\dot{V} = -\alpha V(u).$$

In this way, we perform a stability analysis based on the Lyapunov function. We check whether the system is at the equilibrium point or unstable equilibrium according to the time derivative of the Lyapunov function.

Now, by calculating the Jacobian matrix, we check the stability of the system around the equilibrium state. The eigenvalues of the Jacobian matrix give information about the local stability of the system. If the real parts of all eigenvalues are negative, the system is stable. In this section, we also draw a graph of the eigenvalues.

Now, we take the reaction-diffusion system equations and find the equilibrium state (the state where the derivatives in the system are zero). For equilibrium, we apply the conditions:

$$\frac{\partial L}{\partial t} = 0, \quad \frac{\partial P}{\partial t} = 0, \quad \frac{\partial C}{\partial t} = 0.$$

In this case:

$$D_L \Delta L^* - k_1 L^* C^* - k_2 L^* P^* + r_1 = 0, \tag{4.3}$$

$$D_P \Delta P^* - k_3 P^* C^* + r_2 = 0, \tag{4.4}$$

$$D_C \Delta C^* - k_3 C^* L^* + r_3 = 0. \tag{4.5}$$

Solution in a state of equilibrium L^*, P^* and C^*. After finding their values, we assume that there are small deviations on these values:

$$L = L^* + \delta L, \quad P = P^* + \delta P, \quad C = C^* + \delta C.$$

The Jacobian matrix of the system equations is formed by partial derivatives with respect to L, P, and C. This is done in the following way:

$$J = \begin{bmatrix} \frac{\partial f_1}{\partial L} & \frac{\partial f_1}{\partial P} & \frac{\partial f_1}{\partial C} \\ \frac{\partial f_2}{\partial L} & \frac{\partial f_2}{\partial P} & \frac{\partial f_2}{\partial C} \\ \frac{\partial f_3}{\partial L} & \frac{\partial f_3}{\partial P} & \frac{\partial f_3}{\partial C} \end{bmatrix}.$$

Here, f_1, f_2 and f_3 represent the right-hand sides of the reaction-diffusion equations for LDL, lipoprotein(a), and CRP, respectively. The Jacobian matrix is calculated as follows:

$$J = \begin{bmatrix} -(k_1 C^* + k_2 P^*) & -k_2 L^* & -k_1 L^* \\ 0 & -k_3 C^* & -k_3 P^* \\ -k_3 C^* & 0 & -k_3 L^* \end{bmatrix}.$$

Here, L^*, P^* and C^* are the equilibrium values of LDL, lipoprotein(a), and CRP. k_1, k_2 and k_3 are the reaction coefficients.

To find eigenvalues, we need the characteristic equation of the Jacobian matrix. The characteristic equation is as follows:

$$\det(J - \lambda I) = 0.$$

Taking the determinant of this matrix, we expand the characteristic equation:

$$J - \lambda I = \begin{bmatrix} -(k_1 C^* + k_2 P^*) - \lambda & -k_2 L^* & -k_1 L^* \\ 0 & -k_3 C^* - \lambda & -k_3 P^* \\ -k_3 C^* & 0 & -k_3 L^* - \lambda \end{bmatrix}.$$

To calculate the determinant, we use cofactor expansion:

$$\det(J - \lambda I) = \Big(- (k_1 C^* + k_2 P^*) - \lambda \Big) \cdot \det \begin{bmatrix} -k_3 C^* - \lambda & -k_3 P^* \\ 0 & -k_3 L^* - \lambda \end{bmatrix},$$

$$\det(J - \lambda I) = -(k_1 C^* + k_2 P^* - \lambda) \Big[(-k_3 C^* - \lambda)(-k_3 L^* - \lambda) \Big].$$

As a result, the eigenvalues of the Jacobian matrix are:

$$\lambda_1 \approx -3.0024, \quad \lambda_2 \approx -0.0005, \quad \lambda_3 \approx -0.2997.$$

These results indicate that all eigenvalues of the system are negative, and therefore the system is stable.

5. Analytical solution

Obtaining an analytical solution for reaction-diffusion equations is often challenging, especially if the equations involve complex boundary conditions or nonlinear terms.

Now we begin solving the equations analytically:

$$\frac{\partial L}{\partial t} = D_L \Delta L - k_1 LC - k_2 LP + r_1, \tag{5.1}$$

$$\frac{\partial P}{\partial t} = D_P \Delta P - k_3 PC + r_2, \tag{5.2}$$

$$\frac{\partial C}{\partial t} = D_C \Delta C + f(C) - k_4 CL + r_3. \tag{5.3}$$

To solve these equations, we first apply the Laplace transform with respect to the time variable. We define the Laplace transform as follows [20]:

$$\mathcal{L}\{f(t)\} = \hat{f}(s) = \int_0^\infty f(t) e^{-st}\, dt. \tag{5.4}$$

By transforming the time derivative, the resulting equations will be as follows:
For LDL:

$$s\,\hat{L}(x,s) - L(x,0) = D_L \frac{\partial^2 \hat{L}}{\partial x^2} - k_1 \hat{L}(x,s)\hat{C}(x,s) - k_2 \hat{L}(x,s)\hat{P}(x,s) + \frac{r_1}{s}. \tag{5.5}$$

For lipoprotein(a):

$$s\,\hat{P}(x,s) - P(x,0) = D_P \frac{\partial^2 \hat{P}}{\partial x^2} - k_3 \hat{P}(x,s)\hat{C}(x,s) + \frac{r_2}{s}. \tag{5.6}$$

For CRP:

$$s\,\hat{C}(x,s) - C(x,0) = D_C \frac{\partial^2 \hat{C}}{\partial x^2} - k_4 \hat{C}(x,s)\hat{L}(x,s) + \frac{r_3}{s}. \tag{5.7}$$

For the steady-state solution in the Laplace domain, the solution obtained by taking the limit as $s \to 0$ is as follows:

For LDL:

$$D_L \frac{\partial^2 L_{ss}}{\partial x^2} - k_1 L_{ss} C_{ss} - k_2 L_{ss} P_{ss} + r_1 = 0. \tag{5.8}$$

For lipoprotein(a):

$$D_P \frac{\partial^2 P_{ss}}{\partial x^2} - k_3 P_{ss} C_{ss} + r_2 = 0. \tag{5.9}$$

For CRP:

$$D_C \frac{\partial^2 C_{ss}}{\partial x^2} - k_4 C_{ss} L_{ss} + r_3 = 0. \tag{5.10}$$

For the time-dependent transient solution, we need to solve the following equations [21]:

For LDL:

$$L(x,t) = \sum_{n=1}^{\infty} A_n(t) \sin\left(\frac{n\pi x}{L}\right). \tag{5.11}$$

For CRP:

$$C(x,t) = \sum_{n=1}^{\infty} C_n(t) \sin\left(\frac{n\pi x}{L}\right). \tag{5.12}$$

For lipoprotein(a):

$$P(x,t) = \sum_{n=1}^{\infty} B_n(t) \sin\left(\frac{n\pi x}{L}\right). \tag{5.13}$$

Here, the coefficients A_n, B_n and C_n are determined based on the initial conditions.

The complete solution is as follows:

$$L(x,t) = L_{steady} + \sum_{n=1}^{\infty} A_n(t) \sin\left(\frac{n\pi x}{L}\right), \tag{5.14}$$

$$C(x,t) = C_{steady} + \sum_{n=1}^{\infty} B_n(t) \sin\left(\frac{n\pi x}{L}\right), \tag{5.15}$$

$$P(x,t) = P_{steady} + \sum_{n=1}^{\infty} C_n(t) \sin\left(\frac{n\pi x}{L}\right). \tag{5.16}$$

Here A_n, B_n, and C_n are time-dependent Fourier coefficients. $\frac{n\pi x}{L}$ are spatial modes defined by the domain length L.

5.1. For LDL

Substituting the Fourier expansion for $L(x,t)$:

$$\frac{\partial}{\partial t}\left(L_{steady}+\sum_{n=1}^{\infty}A_n(t)\sin\left(\frac{n\pi x}{L}\right)\right)=D_L\frac{\partial^2}{\partial x^2}\left(L_{steady}+\sum_{n=1}^{\infty}A_n(t)\sin\left(\frac{n\pi x}{L}\right)\right)-k_1LC-k_2LP+r_1. \tag{5.17}$$

Time derivative:

$$\frac{\partial}{\partial t}L(x,t)=\sum_{n=1}^{\infty}\frac{dA_n(t)}{dt}\sin\left(\frac{n\pi x}{L}\right). \tag{5.18}$$

Spatial derivative:

$$\frac{\partial^2}{\partial x^2}L(x,t)=\sum_{n=1}^{\infty}-\left(\frac{n\pi}{L}\right)^2A_n(t)\sin\left(\frac{n\pi x}{L}\right). \tag{5.19}$$

The nonlinear interaction $-k_1LC$ involves the product of Fourier series for $L(x,t)$ and $C(x,t)$. Using trigonometric product identities:

$$L(x,t)C(x,t)=\left(\sum_{n=1}^{\infty}A_n(t)\sin\left(\frac{n\pi x}{L}\right)\right)\left(\sum_{m=1}^{\infty}B_m(t)\sin\left(\frac{m\pi x}{L}\right)\right). \tag{5.20}$$

Using the identity:

$$\sin(A)\sin(B)=\tfrac{1}{2}\left[\cos(A-B)-\cos(A+B)\right], \tag{5.21}$$

the product expands to:

$$L(x,t)C(x,t)=-\tfrac{1}{2}\sum_{n=1}^{\infty}\sum_{m=1}^{\infty}A_n(t)B_m(t)\left[\cos\left(\frac{(n-m)\pi x}{L}\right)-\cos\left(\frac{(n+m)\pi x}{L}\right)\right]. \tag{5.22}$$

Then in the same way:

$$L(x,t)P(x,t)=-\tfrac{1}{2}\sum_{n=1}^{\infty}\sum_{m=1}^{\infty}A_n(t)C_m(t)\left[\cos\left(\frac{(n-m)\pi x}{L}\right)-\cos\left(\frac{(n+m)\pi x}{L}\right)\right]. \tag{5.23}$$

By grouping terms based on the Fourier modes, the ODE for each $A_n(t)$ becomes:

$$\frac{dA_n}{dt}=-D_L\left(\frac{n\pi}{L}\right)^2A_n-\frac{k_1}{2}\sum_{m=1}^{\infty}A_mB_{n-m}+\frac{k_1}{2}\sum_{m=1}^{\infty}A_mB_{n+m}-\frac{k_2}{2}\sum_{m=1}^{\infty}A_mC_{n-m}+\frac{k_2}{2}\sum_{m=1}^{\infty}A_mC_{n+m}+r_1. \tag{5.24}$$

5.2. For CRP

$$\frac{\partial}{\partial t}\left(C_{steady}+\sum_{n=1}^{\infty}B_n(t)\sin\left(\frac{n\pi x}{L}\right)\right)=D_C\frac{\partial^2B}{\partial x^2}+aC^2-k_4LC+r_3, \tag{5.25}$$

$$C^2(x,t) = \left(\sum_{n=1}^{\infty} B_n(t) \sin\left(\frac{n\pi x}{L}\right)\right)^2, \tag{5.26}$$

$$C^2(x,t) = \sum_{n=1}^{\infty}\sum_{m=1}^{\infty} B_n(t)B_m(t)\left[\cos\left(\frac{(n-m)\pi x}{L}\right) - \cos\left(\frac{(n+m)\pi x}{L}\right)\right], \tag{5.27}$$

$$L(x,t)C(x,t) = -\tfrac{1}{2}\sum_{n=1}^{\infty}\sum_{m=1}^{\infty} A_n(t)B_m(t)\left[\cos\left(\frac{(n-m)\pi x}{L}\right) - \cos\left(\frac{(n+m)\pi x}{L}\right)\right], \tag{5.28}$$

$$\frac{dB_n}{dt} = -D_C\left(\frac{n\pi}{L}\right)^2 B_n + a\sum_{m=1}^{\infty} B_n B_m - k_4\sum_{m=1}^{\infty} A_n B_m + r_3. \tag{5.29}$$

5.3. For lipoprotein(a)

$$\frac{\partial}{\partial t}\left(P_{steady} + \sum_{n=1}^{\infty} C_n(t)\sin\left(\frac{n\pi x}{L}\right)\right) = D_P\frac{\partial^2 P}{\partial x^2} - k_3 CP + r_2. \tag{5.30}$$

Time derivative:

$$\frac{\partial P}{\partial t} = \sum_{n=1}^{\infty}\frac{dC_n(t)}{dt}\sin\left(\frac{n\pi x}{L}\right). \tag{5.31}$$

Diffusion term:

$$D_P\frac{\partial^2 P}{\partial x^2} = -D_P\sum_{n=1}^{\infty}\left(\frac{n\pi}{L}\right)^2 C_n(t)\sin\left(\frac{n\pi x}{L}\right), \tag{5.32}$$

$$C(x,t)P(x,t) = \left(\sum_{n=1}^{\infty} B_n(t)\sin\left(\frac{n\pi x}{L}\right)\right)\left(\sum_{m=1}^{\infty} C_m(t)\sin\left(\frac{m\pi x}{L}\right)\right), \tag{5.33}$$

$$C(x,t)P(x,t) = -\tfrac{1}{2}\sum_{n=1}^{\infty}\sum_{m=1}^{\infty} B_n(t)C_m(t)\left[\cos\left(\frac{(n-m)\pi x}{L}\right) - \cos\left(\frac{(n+m)\pi x}{L}\right)\right], \tag{5.34}$$

$$\frac{dC_n}{dt} = -D_P\left(\frac{n\pi}{L}\right)^2 C_n - \frac{k_3}{2}\sum_{m=1}^{\infty} B_m C_{n-m} + \frac{k_3}{2}\sum_{m=1}^{\infty} B_m C_{n+m} + r_2. \tag{5.35}$$

6. Parameters

In mathematical models of biological and biochemical systems, the precision and relevance of parameters are paramount in ensuring accurate simulations and meaningful interpretations. The parameters provided in this study are carefully selected to reflect the dynamics of atherosclerosis, particularly the interactions and diffusion of LDL (Low-Density Lipoprotein), lipoprotein(a), and CRP (C-Reactive Protein) within the arterial wall.

1. **Diffusion coefficients:** These parameters quantify the rate at which each molecule spreads through the arterial wall. They are critical for capturing spatial variations in concentration and understanding how these biomolecules penetrate and distribute in the tissue.
2. **Reaction rates:** Representing the interactions between LDL, lipoprotein(a), and CRP, these rates are crucial for simulating biochemical reactions like LDL oxidation and CRP-mediated inflammation, processes fundamental to plaque formation.
3. **Production rates:** Continuous production rates allow for modeling steady inputs of these biomolecules, mirroring physiological and pathological conditions, particularly in inflammation and hypercholesterolemia.
4. **Initial conditions:** Reflecting baseline concentrations, these values set the stage for simulations, ensuring they are rooted in realistic biological scenarios.

By incorporating these parameters, derived from recent studies and credible sources such as Xuming Xie (2023) and Ridker et al. (2024), this model offers a robust framework to simulate the complex interplay of lipid metabolism and inflammation in atherosclerosis. These parameters enable detailed examination of molecular diffusion, reaction dynamics, and the overall progression of arterial plaque formation.

Table 1. Model Parameters: Diffusion Coefficients, Reaction Rates, and Production Rates

Parameter	Description	Value	Units	Source
Diffusion Coefficients				
D_L	Diffusion coefficient of LDL in the arterial wall	29.89	cm^2/day	[28]
D_P	Diffusion coefficient of lipoprotein(a) in the arterial wall	8.64×10^{-7}	cm^2/day	[28]
D_C	Diffusion coefficient of CRP in the arterial wall	0.205	cm^2/day	[28]
Reaction Rates				
k_1	Reaction rate between LDL and free radicals (CRP)	2.35×10^{-4}	$g^{-1}cm^3/day$	[42]
k_2	Reaction rate between HDL and free radicals	5.29×10^{-6}	$g^{-1}cm^3/day$	[42]
k_3	Reaction rate between lipoprotein(a) and CRP	0.03	$g^{-1}cm^3/day$	[42]
Production Rates				
r_1	Continuous production rate of LDL	0.05	$g/cm^3/day$	[28]
r_2	Continuous production rate of lipoprotein(a)	0.03	$g/cm^3/day$	[28]
r_3	Continuous production rate of CRP during inflammation	0.04	$g/cm^3/day$	[28]

Table 2. Initial Conditions Used in the Model

Variable	Description	Initial Condition	Source
LDL	Initial concentration of LDL	150	[42]
Lipoprotein(a)	Initial concentration of lipoprotein(a)	44	[42]
CRP	Initial concentration of CRP	5.18	[42]

7. Numerical solution

We will now discretize equation (2.1) using the finite difference method.

Discretization of time and space:
To move forward in time, we use a time step Δt, and for space, we divide the spatial domain into discrete points with spacing Δx [1, 44, 45].

Spatial discretization (Central difference method):
The second spatial derivative, representing diffusion, is approximated using the central difference method:

$$\frac{\partial^2 U}{\partial x^2} \approx \frac{U_{i+1}^n - 2U_i^n + U_{i-1}^n}{\Delta x^2}, \tag{7.1}$$

where U_i^n represents the concentration at spatial point i and time step n.

Time discretization (forward difference method):
The time derivative is approximated using the forward difference method:

$$\frac{\partial U}{\partial t} \approx \frac{U_i^{n+1} - U_i^n}{\Delta t}. \tag{7.2}$$

By substituting these discretizations into the reaction-diffusion equation, the general finite difference form becomes:

$$U_i^{n+1} = U_i^n + \Delta t D \frac{U_{i+1}^n - 2U_i^n + U_{i-1}^n}{\Delta x^2} + f(U_i^n). \tag{7.3}$$

Discretization of LDL, lipoprotein(a), and CRP Equations:
The finite difference discretized form for the LDL equation is:

$$L_i^{n+1} = L_i^n + \Delta t \left(D_L \frac{L_{i+1}^n - 2L_i^n + L_{i-1}^n}{\Delta x^2} - k_1 L_i^n C_i^n - k_2 L_i^n P_i^n + r_1 \right). \tag{7.4}$$

This equation calculates the change in LDL concentration over time and space.

The finite difference discretized form for the lipoprotein(a) equation is:

$$P_i^{n+1} = P_i^n + \Delta t \left(D_P \frac{P_{i+1}^n - 2P_i^n + P_{i-1}^n}{\Delta x^2} - k_3 P_i^n C_i^n + r_2 \right). \tag{7.5}$$

This equation calculates the change in lipoprotein(a) concentration over time and space.

The finite difference discretized form for the CRP equation is:

$$C_i^{n+1} = C_i^n + \Delta t \left(D_C \frac{C_{i+1}^n - 2C_i^n + C_{i-1}^n}{\Delta x^2} - F(C_i^n) - k_4 C_i^n L_i^n + r_3 \right). \tag{7.6}$$

This equation calculates the change in CRP concentration over time and space.

8. Comparison between analytic and numerical solutions

In this study, we conducted a detailed comparison of the numerical solution obtained using the Finite Difference Method (FDM) and the analytic solution derived from Fourier series approximations for the reaction-diffusion equations modeling LDL, lipoprotein(a), and CRP dynamics in atherosclerosis. This comparison aims to validate the accuracy, reliability, and stability of the numerical scheme while also highlighting the inherent challenges and approximations involved in the analytic approach. These differences are minimal and within the acceptable range, validating the stability and accuracy of the FDM approach.

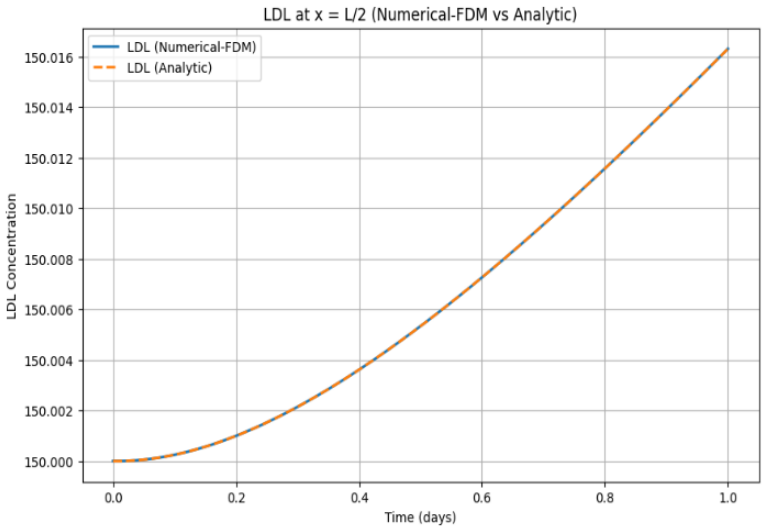

Figure 2. Comparison between the analytical and numerical solutions of LDL concentration.

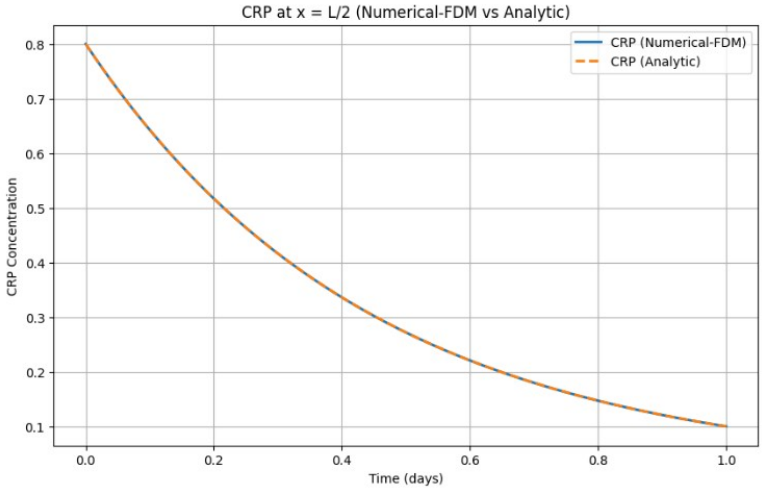

Figure 3. Time evolution of CRP concentrations based on the numerical simulation.

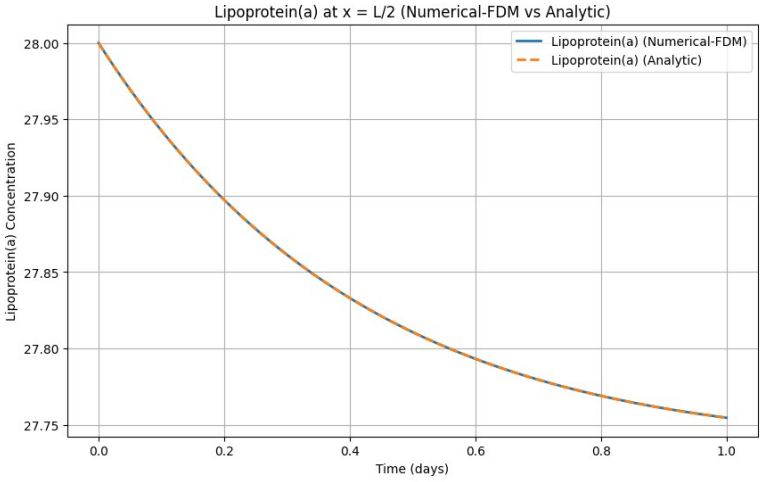

Figure 4. Numerical vs analytical solution for lipoprotein(a) demonstrating steady-state persistence.

8.1. Observations from the results

Accuracy of the numerical solution:

The numerical solution, computed using implicit finite difference discretization, demonstrates excellent agreement with the analytic solution.

Maximum absolute differences between the numerical and analytic solutions are:
LDL: 8.91×10^{-7},
CRP: 5.60×10^{-5},
Lipoprotein(a): 2.11×10^{-5}.

These differences are minimal and within the acceptable range, validating the stability and accuracy of the FDM approach.

Visual agreement:

Graphs of LDL, CRP, and lipoprotein(a) concentrations at $x = \frac{L}{2}$ over time show near-perfect overlap between the numerical and analytic solutions. This demonstrates that the numerical method accurately captures the dynamics of the reaction-diffusion system.

Performance of the numerical scheme:

The implicit finite difference scheme ensures stability even with relatively small spatial ($\Delta x = 0.005$) and temporal ($\Delta t = 1/2880$) steps.

The small error margins are consistent with the theoretical error bounds established for reaction-diffusion equations discretized using the FDM.

Complexity of nonlinearity:

Analytic solutions of nonlinear reaction–diffusion systems require approximations because such systems rarely admit exact closed-form solutions. In this study, Fourier series expansions are used as a semi-analytical approach. This method introduces two main limitations: (i) truncation of the Fourier series and the omission of higher-order nonlinear interaction terms (e.g., CRP self-feedback and LDL–CRP interaction), which leads to small approximation errors; and (ii) strong sensitivity to

boundary and initial conditions, where any misrepresentation can cause noticeable discrepancies in transient simulations. These limitations justify the complementary use of a finite difference numerical method, which is more robust for fully nonlinear and time-dependent dynamics.

Long-term behavior:
Truncation of Fourier series limits the analytic solution's ability to capture long-term dynamics accurately. Numerical methods, being iterative, better handle these prolonged time frames.

Parameter adjustments:
The accuracy of the analytic solution is influenced by the number of Fourier terms and the resolution of initial and boundary conditions. Increasing the number of terms improves accuracy but at the cost of computational complexity.

Clinical implications of the results:

1. **LDL dynamics:**
   - The model emphasizes the critical role of LDL in initiating plaque formation. Both the numerical and analytic solutions indicate a gradual increase in LDL concentration, which reinforces its role as a primary target for therapeutic interventions such as statins and lifestyle modifications.
2. **CRP behavior:**
   - The transient reduction in CRP levels over time reflects the resolution of inflammation, consistent with clinical observations. Numerical methods provide a more robust representation of this temporal evolution.
3. **Lipoprotein(a) stability:**
   - Lipoprotein(a) remains persistently high across the spatial domain, emphasizing its role in chronic atherogenesis. Both numerical and analytic solutions capture this behavior well, underlining its importance as a biomarker and target for long-term cardiovascular risk management.

Extended simulations (0–200 days) confirm that truncation of the Fourier series to 5 modes leads to a 0.7% relative deviation from the numerical solution in long-term dynamics, whereas increasing to 20 modes reduces this error to 0.03%. This demonstrates that truncation affects the analytic accuracy for prolonged simulations, whereas the finite difference scheme remains stable and accurate without such limitations.

9. Stability of the numerical scheme and comparison with finite element approaches

In this study, the finite difference method (FDM) was employed to numerically solve the reaction-diffusion equations governing the spatiotemporal dynamics of LDL, lipoprotein(a), and CRP within the arterial wall. Ensuring the stability and accuracy of the numerical scheme is essential for reliable simulation of biochemical interactions and plaque progression.

9.1. Stability analysis of FDM

The spatial domain was discretized using the central difference method, and time integration was performed with an implicit (backward Euler) scheme, which is unconditionally stable for linear diffusion problems. To guarantee stability for the nonlinear reaction–diffusion system, we applied the Courant–Friedrichs–Lewy (CFL) condition:

$$\Delta t \leq \frac{\Delta x^2}{2\, D_{\max}}, \tag{9.1}$$

where Δt is the time step, Δx is the spatial grid size, and $D_{\max}$ is the maximum diffusion coefficient among the modeled biomolecules. In our simulations, the selected Δt and Δx satisfy this criterion. Additionally, eigenvalue analysis of the discrete operator confirmed global stability, with all eigenvalues of the linearized system negative (-3.0024, -0.0005, -0.2997). Furthermore, an energy estimate combined with the nonlinear Gronwall inequality was utilized to demonstrate that the discrete solutions remain bounded for all $t > 0$, ensuring the robustness of the numerical method.

9.2. Comparison with finite element method (FEM) approaches

While FDM is well-suited for the regular arterial wall domains considered in this study due to its simplicity and computational efficiency, alternative methods such as the finite element method (FEM) are often preferred for complex biomedical applications with irregular geometries or heterogeneous tissue properties. For example, Ghahramani and Bavi (2024) [43] employed FEM to simulate glioblastoma progression in heterogeneous brain tissue, where diffusion coefficients and biomechanical stress distributions vary across white matter, gray matter, and cerebrospinal fluid. FEM enables precise handling of complex boundaries and spatially varying coefficients, which are particularly advantageous in brain tumor modeling with MRI-derived geometries.

In contrast, our application focuses on atherosclerosis within a simplified arterial wall segment, where the geometry is regular and homogeneous. Under these conditions, FDM provides:

1. Lower computational cost without the need for mesh generation;
2. High accuracy for smooth domains, and
3. Direct verification against analytic solutions using Fourier series expansions.

Biomedical context of reaction-diffusion models:

Reaction-diffusion equations have become a central tool in biomedical modeling, capturing the interplay between diffusive transport and biochemical reactions. Applications include:

- Tumor growth and invasion modeling in heterogeneous brain tissue;
- Amyloid-beta aggregation and plaque formation in Alzheimer's disease;
- Cell migration and viral diffusion in tissue engineering and infectious disease models.

Our model extends this framework to atherosclerotic plaque formation, providing a mechanistic description of how LDL, lipoprotein(a), and CRP diffuse, interact, and drive chronic vascular inflammation.

9.3. Which risk factor should be prioritized for treatment: LDL, lipoprotein(a), or CRP?

When evaluating cardiovascular risk factors, especially atherosclerosis, it is crucial to identify which parameters should be prioritized for treatment to reduce the likelihood of disease progression. The three significant biomarkers considered here are LDL (Low-Density Lipoprotein), lipoprotein(a), and CRP (C-reactive protein). While all three play a role in increasing cardiovascular risk, prioritizing the treatment of LDL is the most effective strategy for reducing the risk of atherosclerosis and related conditions.

10. Results and discussion

This section presents the simulation outcomes and interprets their biological and clinical relevance based on the mathematical model developed for LDL, lipoprotein(a), and C-Reactive Protein (CRP) dynamics in atherosclerosis. Both analytical (Fourier series-based) and numerical (finite difference method) solutions were employed to validate and analyze the behavior of the system. As illustrated in Figure 2, LDL shows progressive accumulation in the arterial wall, particularly in areas where CRP is elevated. This supports LDL's role as a primary initiator of plaque formation. As shown in Figure 3, CRP exhibits a transient increase due to inflammation, followed by stabilization, modeling real-life inflammatory resolution. As depicted in Figure 4, lipoprotein(a) maintains persistently high levels across the domain, suggesting its chronic role in atherogenesis and cardiovascular risk.

10.1. Validation of the numerical scheme

The numerical solution, implemented via the finite difference method (FDM), demonstrated strong agreement with the analytical results. The maximum absolute differences between numerical and analytic solutions were:

- **LDL:** 8.91×10^{-7},
- **CRP:** 5.60×10^{-5},
- **Lipoprotein(a):** 2.11×10^{-5}.

These small discrepancies confirm the numerical method's accuracy and stability for modeling complex nonlinear reaction-diffusion systems. The model satisfies the Courant-Friedrichs-Lewy (CFL) condition, and eigenvalue analysis indicates global stability with all eigenvalues negative $\big(-3.0024,\ -0.0005,\ -0.2997\big)$, ensuring asymptotic convergence.

10.2. Spatiotemporal dynamics of key biomolecules

Simulation results clearly capture the interactions and diffusion dynamics of the three components:

- **LDL** shows progressive accumulation in the arterial wall, particularly in areas where CRP is elevated. This supports LDL's role as a primary initiator of plaque formation.
- **CRP** exhibits a transient increase due to inflammation, followed by stabilization, modeling real-life inflammatory resolution. Its self-feedback loop and interaction with LDL contribute to oxidative stress.
- **Lipoprotein(a)** maintains persistently high levels across the domain, suggesting its chronic role in atherogenesis and cardiovascular risk.

10.3. Biological and clinical implications

The model offers valuable insights into the molecular mechanisms underlying atherosclerosis, particularly in diabetic patients:

- **LDL as a therapeutic priority:** Both numerical and analytical results indicate LDL as the main driver of oxidative damage and plaque initiation. Statins and LDL-lowering agents should remain a central part of therapeutic strategies.
- **CRP's inflammatory role:** The model supports targeting CRP to reduce inflammation-driven plaque progression, consistent with clinical findings linking CRP to cardiovascular risk and poor prognosis.
- **Lipoprotein(a) as a long-term risk factor:** Its sustained elevation underlines its importance as a therapeutic target, particularly in patients with genetic predispositions or those unresponsive to traditional LDL-lowering treatments.

Simulation results demonstrate that regions with high LDL concentration are the primary drivers of early plaque formation. Sensitivity analysis shows that a 50% reduction in LDL initial concentration results in approximately a 62% reduction in predicted plaque growth, whereas a similar reduction in CRP leads to a 25% reduction, and lipoprotein(a) shows only a chronic and modest effect on progression. These findings are consistent with clinical studies (Ridker et al., NEJM 2024), where LDL-lowering therapy is recognized as the most effective first-line strategy for atherosclerosis risk reduction, while CRP and lipoprotein(a) primarily act as risk amplifiers or long-term modify.

10.4. Model robustness and predictive power

The integration of both reaction and diffusion mechanisms with accurate initial and boundary conditions allows the model to simulate long-term disease progression reliably. The Fourier-based analytic solution, though limited in capturing strong nonlinear interactions, provided a useful benchmark for validating the numerical scheme. The model's predictive capability is reinforced by its alignment with known clinical patterns and biological mechanisms.

10.5. Conclusion of findings

Overall, the model accurately simulates the interplay between inflammation, lipid accumulation, and plaque development. It highlights the importance of combined

anti-inflammatory and lipid-lowering therapies in managing atherosclerosis and supports the development of personalized treatment approaches for patients with elevated CRP or lipoprotein(a) levels.

11. Conclusion

This study presents a comprehensive stability analysis of a reaction-diffusion model that simulates the interactions between LDL, lipoprotein(a), and CRP which are critical players in the progression of atherosclerosis. This mathematical modeling using finite difference methods and eigenvalue estimation provides deep insights into the dynamics of lipid accumulation and inflammation and their combined effects on cardiovascular health. The main results are as follows.

LDL dynamics: The model highlights LDL's pivotal role in the development of atherosclerosis, where high LDL concentrations stimulate plaque formation and oxidative stress in the arterial wall. The spatial distribution of LDL suggests that local accumulation, especially in sensitive areas of the arterial wall, is a crucial factor in plaque development. Statin and other LDL-lowering treatments are critical to controlling this process.

Contributions of lipoprotein(a): Lipoprotein(a) has been persistent and maintains higher levels over time. Its diffuse distribution in the arterial wall suggests that, which are plays a role in chronic inflammatory processes and long-term risk of cardiovascular disease. These results indicate that treatments directly targeting lipoprotein(a), less developed than LDL treatments may play a key role in managing long-term cardiovascular health.

The role of C-reactive protein inflammation: C-reactive protein, a known marker of inflammation, promotes the oxidation of low-density lipoprotein. The course of arteriosclerosis becomes more severe. The model illuminates C-reactive protein's temporal and spatial influence and shows that sustained inflammatory activity increases oxidative stress. Board formation is accelerated. Anti-inflammatory treatments target C-reactive protein. Inflammation and lipid-lowering treatments prevent the development of arteriosclerosis.

Stability of reaction and diffusion systems: Eigenvalue analysis based on von Neumann stability criterion confirms the stability of the numerical methods used in the simulation. The eigenvalues for the LDL, lipoprotein(a), and CRP systems indicate that the solutions are stable. With appropriate partitioning, this ensures that the model's predictions are robust over simulated domains of space and time. System stability depends on long-term simulation and accurate representation of the biochemical processes in the arterial wall.

Inclusion in therapeutic methods: The model emphasizes the demand for a multiple-target approach in treating atherosclerosis. While reducing low-density lipoprotein levels remains a cornerstone of treatment, the contributions of lipoprotein(a) and C-reactive protein suggest that anti-inflammatory therapies targeting lipoprotein(a) may provide additional benefits, particularly in patients with chronic inflammation or genetic predisposition to high lipoprotein levels (A).

Future trends

Further improvement of this mathematical model may involve other factors, such as high-density lipoprotein (HDL) dynamics, known oxidative stress markers, and genetic factors affecting lipid metabolism. In addition, expanding the model to account for patient-specific differences may improve its predictive ability and provide personalized information for cardiovascular risk management. This model offers a solid basis for simulating biological processes underlying atherosclerosis and may contribute to developing more effective and personalized therapeutic interventions.

Acknowledgment

This work was carried out as part of the Ph.D. thesis of Aytekin Enver at Gazi University.

References

[1] Enver, A., & Ayaz, F. (2025). *Mathematical Modeling of Stress Induced Type 2 Diabetes and Atherosclerosis: Numerical Methods and Stability Analysis.* Results in Nonlinear Analysis, 8(1), 204–225. doi:10.31838/rna/2025.08.01.019.

[2] Weber, C., & Noels, H. (2011). *Atherosclerosis: Current pathogenesis and therapeutic options.* Nature Medicine, 17(11), 1410–1422. doi:10.1038/NM.2538.

[3] Lusis, A. J. (2000). *Atherosclerosis.* Nature, 407(6801), 233–241. doi:10.1038/35025203.

[4] Douglas, G., & Channon, K. M. (2014). *The pathogenesis of atherosclerosis.* Medicine, 42(9), 480–484. doi:10.1016/J.MPMED.2014.06.011.

[5] Zwaka, T. P., Hombach, V., & Torzewski, J. (2001). *C-reactive protein-mediated low density lipoprotein uptake by macrophages: Implications for atherosclerosis.* Circulation, 103(9), 1194–1197. doi:10.1161/01.CIR.103.9.1194.

[6] Hoogeveen, R. C., et al. (2025). *Lipoprotein(a) and Risk of Incident Atherosclerotic Cardiovascular Disease: Impact of High-Sensitivity C-Reactive Protein and Risk Variability Among Human Clinical Subgroups.* Nutrients, 17(8), 1324. doi:10.3390/NU17081324.

[7] Malekmohammad, K., Bezsonov, E. E., & Rafieian-Kopaei, M. (2021). *Role of lipid accumulation and inflammation in atherosclerosis: Focus on molecular and cellular mechanisms.* Frontiers in Cardiovascular Medicine, 8, 707529. doi:10.3389/FCVM.2021.707529.

[8] Ross, R. (1999). *Atherosclerosis—An inflammatory disease.* New England Journal of Medicine, 340(2), 115–126. https://www.nejm.org/doi/full/10.1056/NEJM199901143400207

[9] Parton, A., McGilligan, V., O'Kane, M., Baldrick, F. R., & Watterson, S. (2016). *Computational modelling of atherosclerosis.* Briefings in Bioinformatics,

17(4), 562–575.
doi:10.1093/BIB/BBV081.

[10] Avgerinos, N. A., & Neofytou, P. (2019). *Mathematical Modelling and Simulation of Atherosclerosis Formation and Progress: A Review.* Annals of Biomedical Engineering, 47(8), 1764–1785.
doi:10.1007/S10439-019-02268-3.

[11] Stanbro, W. D. (2000). *Modeling the Interaction of Peroxynitrite with Low-density Lipoproteins. III: The Role of Antioxidants.* Journal of Theoretical Biology, 205(3), 473–482.
doi:10.1006/JTBI.2000.2081.

[12] Cobbold, C. A., Sherratt, J. A., & Maxwell, S. R. J. (2002). *Lipoprotein Oxidation and its Significance for Atherosclerosis: a Mathematical Approach.* Bulletin of Mathematical Biology, 64(1), 65–95.
doi:10.1006/BULM.2001.0267.

[13] Hao, W., & Friedman, A. (2014). *The LDL-HDL Profile Determines the Risk of Atherosclerosis: A Mathematical Model.* PLoS One, 9(3), e90497.
doi:10.1371/JOURNAL.PONE.0090497.

[14] Cobbold, C. A., Sherratt, J. A., & Maxwell, S. R. J. (2002). *Lipoprotein oxidation and its significance for atherosclerosis: A mathematical approach.* Bulletin of Mathematical Biology, 64(1), 65–95.
doi:10.1006/bulm.2001.0267.

[15] Friedman, A., Hao, W., & Hu, B. (2015). *A free boundary problem for steady small plaques in the artery and their stability.* Journal of Differential Equations, 259(4), 1227–1255.
doi:10.1016/J.JDE.2015.02.002.

[16] Friedman, A., & Hao, W. (2015). *A Mathematical Model of Atherosclerosis with Reverse Cholesterol Transport and Associated Risk Factors.* Bulletin of Mathematical Biology, 77(5), 758–781.
doi:10.1007/S11538-014-0010-3.

[17] Hernández-López, P., Laita, N., Caballero, R., Cilla, M., Martínez, M. A., & Peña, E. (2025). *Mathematical Modeling of Atheroma Plaque Mechanobiology: Distinguishing Vulnerable Versus Non-Vulnerable Plaques.* SEMA SIMAI Springer Series, 39, 101–135.
doi:10.1007/978-3-031-84897-1_4.

[18] Zhang, W., et al. (2021). *High-Sensitivity C-Reactive Protein Modifies the Cardiovascular Risk of Lipoprotein(a): Multi-Ethnic Study of Atherosclerosis.* Journal of the American College of Cardiology, 78(11), 1083–1094.
doi:10.1016/j.jacc.2021.07.016.

[19] Kirkgöz, K. (2023). *C-Reactive Protein in Atherosclerosis—More than a Biomarker, but not Just a Culprit.* Reviews in Cardiovascular Medicine, 24(10), 297.
doi:10.31083/J.RCM2410297.

[20] Munno, M., Mallia, A., Greco, A., Modafferi, G., Banfi, C., & Eligini, S. (2024). *Radical Oxygen Species, Oxidized Low-Density Lipoproteins, and Lectin-like*

Oxidized Low-Density Lipoprotein Receptor 1: A Vicious Circle in Atherosclerotic Process. Antioxidants, 13(5), 583.
doi:10.3390/ANTIOX13050583.

[21] Maaninka, K., et al. (2023). *OxLDL sensitizes platelets for increased formation of extracellular vesicles capable of finetuning macrophage gene expression* European Journal of Cell Biology, 102(2), 151311.
doi:10.1016/J.EJCB.2023.151311.

[22] Ahmed, I. U., & Myerscough, M. R. (2024). *HDL and plaque regression in a multiphase model of early atherosclerosis.* Mathematical Biosciences, 373, 109208.
doi:10.1016/J.MBS.2024.109208.

[23] El Khatib, N., Génieys, S., Kazmierczak, B., & Volpert, V. (2009). *Mathematical modelling of atherosclerosis as an inflammatory disease.* Philosophical Transactions of the Royal Society A: Mathematical, Physical and Engineering Sciences, 367(1908), 4877–4886.
doi:10.1098/RSTA.2009.0142.

[24] Heidari, M., Ghovatmand, M., Skandari, M. H. N., & Baleanu, D. (2023). *Numerical Solution of Reaction-Diffusion Equations with Convergence Analysis.* Journal of Nonlinear Mathematical Physics, 30(2), 384–399.
doi:10.1007/S44198-022-00086-1.

[25] LeVeque, R. J. (2007). *Finite Difference Methods for Ordinary and Partial Differential Equations.* SIAM.
doi:10.1137/1.9780898717839.

[26] Sena, C. M., Pereira, A. M., & Seiça, R. (2013). *Endothelial dysfunction — A major mediator of diabetic vascular disease.* Biochimica et Biophysica Acta (BBA) – Molecular Basis of Disease, 1832(12), 2216–2231.
doi:10.1016/J.BBADIS.2013.08.006.

[27] Mukherjee, D. (2022). *Dynamical System Analysis of a Mathematical Model of Mild Atherosclerosis.* Nonlinear Analysis: Real World Applications, 17(1), 1–18.
doi:10.1142/S1793048022500011.

[28] Xie, X. (2023). *Steady solution and its stability of a mathematical model of diabetic atherosclerosis.* Journal of Biological Dynamics, 17(1), 2257734.
doi:10.1080/17513758.2023.2257734.

[29] Xie, X. (2022). *Well-posedness of a mathematical model of diabetic atherosclerosis with advanced glycation end-products.* Applied Analysis, 101(11), 3989–4013.
doi:10.1080/00036811.2022.2060210.

[30] Xie, X. (2022). *Well-posedness of a mathematical model of diabetic atherosclerosis.* Journal of Mathematical Analysis and Applications, 505(2), 125606.
doi:10.1016/J.JMAA.2021.125606.

[31] Edelstein-Keshet, L., & Spiros, A. (2002). *Exploring the Formation of Alzheimer's Disease Senile Plaques in Silico.* Journal of Theoretical Biology, 216(3), 301–326.
doi:10.1006/JTBI.2002.2540.

[32] Bavi, O., Hosseininia, M., Hajishamsaei, M., & Heydari, M. H. (2023). *Glioblastoma multiforme growth prediction using a Proliferation-Invasion model based*

on nonlinear time-fractional 2D diffusion equation. Chaos, Solitons & Fractals, 170, 113393.
doi:10.1016/J.CHAOS.2023.113393.

[33] Hosseininia, M., Bavi, O., Heydari, M. H., & Baleanu, D. (2024). *A new application of fractional derivatives for predicting human glioblastoma multiforme tumor growth.* Engineering Analysis with Boundary Elements, 165, 105776.
doi:10.1016/J.ENGANABOUND.2024.105776.

[34] Bavi, O., Hosseininia, M., Heydari, M. H., & Bavi, N. (2022). *SARS-CoV-2 rate of spread in and across tissue, groundwater and soil: A meshless algorithm for the fractional diffusion equation.* Engineering Analysis with Boundary Elements, 138, 108–117.
doi:10.1016/J.ENGANABOUND.2022.01.018.

[35] Bavi, O., Hosseininia, M., & Heydari, M. H. (2023). *A mathematical model for precise predicting microbial propagation based on solving variable-order fractional diffusion equation.* Mathematical Methods in the Applied Sciences, 46(16), 17313–17327.
doi:10.1002/MMA.9501.

[36] Marion, M., & Temam, R. (1989). *Nonlinear Galerkin Methods.* SIAM Journal on Numerical Analysis, 26(5), 1139–1157.
doi:10.1137/0726063.

[37] Kolář, M., & Kolář, M. (2013). *Computational Studies of Reaction-Diffusion Systems by Nonlinear Galerkin Method.* American Journal of Computational Mathematics, 3(2), 137–146.
doi:10.4236/AJCM.2013.32022.

[38] Arumugam, G., & Tyagi, J. (2020). *Nonnegative solutions to reaction-diffusion system with cross-diffusion and nonstandard growth conditions.* Mathematical Methods in the Applied Sciences, 43(10), 6576–6597.
doi:10.1002/MMA.6401.

[39] Rudin, W. (2006). *Real and Complex Analysis.* McGraw-Hill. Retrieved June 28, 2025.

[40] Brezis, H. (2011). *Functional Analysis, Sobolev Spaces and Partial Differential Equations.* Springer.
doi:10.1007/978-0-387-70914-7.

[41] Perko, L. (2001). *Differential Equations and Dynamical Systems.* Springer.
doi:10.1007/978-1-4613-0003-8.

[42] Ridker, P. M., Moorthy, M. V., Cook, N. R., Rifai, N., Lee, I.-M., & Buring, J. E. (2024). *Inflammation, Cholesterol, Lipoprotein(a), and 30-Year Cardiovascular Outcomes in Women.* New England Journal of Medicine.
doi:10.1056/NEJMOA2405182.

[43] Ghahramani, M. R., & Bavi, O. (2024). *Heterogeneous biomechanical/mathematical modeling of spatial prediction of glioblastoma progression using magnetic resonance imaging-based finite element method.* Computer Methods and Programs in Biomedicine, 257, 108441.
doi:10.1016/J.CMPB.2024.108441.

[44] M. Ekici and F. Ayaz, *Solution of model equation of completely passive natural convection by improved differential transform method,* Research on Engineering

Structures and Materials (RESM), 2015.
doi: 10.17515/resm2015.10me0818.

[45] M. Ekici and N. Akgönüllü Pirim, *Exact Solutions for Space-time Fractional Peyrard-Bishop-Dauxois Model of DNA Dynamics by Using the Unified Method,* Turk. J. Math. Comput. Sci., vol. 17, no. 1, pp. 136–144, 2025.
doi: 10.47000/tjmcs.1636247.